

# A Spectroscopic Study of HL Canis Majoris <sup>1</sup>

H. A. Sheets and John R. Thorstensen

*Department of Physics and Astronomy  
6127 Wilder Laboratory, Dartmouth College  
Hanover, NH 03755-3528;  
h.a.sheets@dartmouth.edu*

## ABSTRACT

We present optical spectroscopy of the dwarf nova HL Canis Majoris over a span of four years. The observations were made during standstill, outburst, and quiescence. We determine an orbital period of  $0.2167867 \pm 0.0000017$  days, based on radial velocities determined from  $H\alpha$ ,  $H\beta$ , and  $HeI \lambda 5876$  emission. We also present equivalent widths of the spectral features in outburst and in quiescence.

*Subject headings:* stars: dwarf novae – stars: individual (HL CMa)

## 1. Introduction

HL Canis Majoris, despite being one of the brightest dwarf novae, was long overlooked because of its location in the sky 9 arcminutes south of Sirius. HL CMa was first detected when observations of Sirius by *Einstein* showed a nearby X-ray source, whose location matched that of a variable star on plates from the Harvard archive (Chlebowski et al. 1981); subsequent optical photometry and spectroscopy exhibited characteristics typical of dwarf novae, such as recurring outbursts on an approximately 15-day cycle and Balmer emission lines. Further photometric study revealed standstills in 1982 and 1999 (Watanabe et al. 2000) that led to the further classification of HL CMa as a Z Cam star. In 2001, the variable also exhibited an unusual outburst cycle of roughly 30 days (Kato 2002).

A spectroscopic study of HL CMa by Hutchings et al. (1981) gave an orbital period of either 0.22 or 0.18 d. They obtained spectra during both outburst and quiescence and found no conclusive evidence in their data for orbital phase-dependent phenomena. Wargau et al. (1983) then studied optical spectra of the rise to outburst, maximum, and decline from outburst. They found a period of  $0.2145(4)$  d <sup>2</sup> and noted absorption wings around the Balmer and  $HeI$  lines. Most recently, Still

---

<sup>1</sup>Based on observations obtained at the MDM Observatory, operated by Dartmouth College, Columbia University, Ohio State University, and the University of Michigan.

<sup>2</sup>Uncertainties in the last quoted digits are given in parentheses.

et al. (1999) have given a period of either 0.2146(4) or 0.2212(5) d, based on data obtained during outburst. They also found that the Balmer lines were composed of a narrow core, brightest as it shifts from red to blue, and a broader component that does not vary greatly in brightness.

After more than two decades of study, HL CMa still lacked a precisely determined orbital period. For this reason, we collected spectra over many runs in order to suppress aliasing and determine the period without ambiguity. In the process of gathering these observations, an improved finding chart was also created which is now available from the Living Edition of the Catalog and Atlas of Cataclysmic Variables (Downes et al. 2001).

## 2. Observations

Spectra of HL Canis Majoris were taken over 14 observing runs between 2000 January and 2004 March from the MDM Observatory at Kitt Peak, Arizona, using mainly the 2.4m Hiltner telescope. The 2001 December data were obtained on the 1.3m McGraw-Hill telescope. The spectra were obtained during both outburst and quiescence. Two spectra, taken in 2000 January, were obtained during the standstill that began in 1999 (Watanabe et al. 2000), and many spectra were obtained during the unusual outburst state in 2001-2002 reported by Kato (2002).

The observation and reduction procedures for the Hiltner telescope data were mostly as described in Thorstensen et al. (2004). In brief, we used the modular spectrograph and a SITe 2048<sup>2</sup> CCD detector, with 2.0 Å pixel<sup>-1</sup> from 4300 to 7500 Å and a spectral resolution of 3.5 Å. The McGraw-Hill observations were made with the Mark III spectrograph and a SITe 1024<sup>2</sup> CCD detector, with 2.2 Å pixel<sup>-1</sup> from 4500 to 6800 Å and a spectral resolution of 5.0 Å. Many comparison Hg-Ne-Xe lamp spectra were taken throughout each night in the runs from January 2000 through October 2003, while the night sky lines were used for the wavelength zero point for the January and March 2004 data. The spectra were then reduced using standard IRAF<sup>3</sup> procedures. We observed flux standard stars when conditions appeared clear, and the flux calibration was checked by calculating the *V* magnitudes from the spectra using the passband tabulated by Bessell (1990). The calculated *V* magnitudes for outburst spectra were between 12.5 and 11.6, similar to the 11.7 given by the Living Edition (Downes et al. 2001), while those of the quiescent spectra were close to 14.0, while the Living Edition gives a magnitude of 14.5. Typically, the flux calibrations for our setup are accurate to approximately 10 to 20 percent, with systematic errors dominating.

---

<sup>3</sup>IRAF is distributed by the National Optical Astronomy Observatories.

### 3. Results

The quiescent spectra show Balmer line emission, as well as HeII  $\lambda 4686$  and several HeI lines, all of which are typical of dwarf novae in quiescence. In outburst, the spectra show broad absorption wings around H $\beta$ , H $\gamma$ , and HeI  $\lambda 5876$ , as noted in previous studies by Wargau et al. (1983) and Still et al. (1999). The CIII/NIII feature also stands out strongly just blueward of HeII  $\lambda 4686$ . This feature is not as clear in the quiescent spectra but seems to be weakly present. Table 1 gives the equivalent widths and FWHM for each state. Figure 1 shows the average of the January 2002 spectra and that of the October 2003 spectra, from which the measurements in Table 1 were determined. The two spectra obtained during standstill, as well as those obtained during the unusual outburst cycle, do not appear to differ significantly from spectra obtained during a normal outburst.

The radial velocities, given in Table 2, were determined from the H $\alpha$  emission line using convolution methods set forth by Schneider & Young (1980) and Shafter (1983). Shafter's technique convolves the spectral line with a positive and a negative Gaussian separated by a given width, instead of the derivative of a Gaussian used by Schneider and Young. We used Gaussians each with a width of 6 Å and separated by 14 Å for our data. The velocities had uncertainties estimated from counting statistics errors of typically 7 km s $^{-1}$  or less. We searched for the orbital frequency using the “residualgram” method (Thorstensen et al. 1996), which gave a well-determined frequency of 4.61282 d $^{-1}$ . The large number of observing runs, coupled with long sequences of observations during those runs, resulted in an unambiguous cycle count over the four-year span of the data set. Figure 2 shows the periodogram of this search. The Monte Carlo test described by Thorstensen & Freed (1985) gives a discriminatory power of 998/1000 for the 4.61282 d $^{-1}$  frequency, which corresponds to an orbital period of 0.216787 d. The velocities, weighted by their uncertainties, were then fit to a sinusoid  $v(t) = \gamma + K \sin[2\pi(t - T_0)/P]$ . The parameters of the fit are given in Table 3, and the folded velocity plot is shown in Figure 3.

While the period we determined is similar to those suggested in previous studies of HL CMa, it still differs from them by more than the margin of error in each. To further ensure that our period is correct, we determined the radial velocities from the H $\alpha$  line using the original convolution method of Schneider & Young (1980), and also determined the velocities from the H $\beta$  and HeI  $\lambda 5876$  lines using both methods. The errors in the velocities from H $\beta$  and HeI  $\lambda 5876$  were typically of the order of 10 to 20 km s $^{-1}$ . The results from the period searches of each set of velocities are listed in Table 3. The H $\beta$  velocities did not independently confirm our choice of cycle count, evidently because of inadequate signal-to-noise, but did show strong power at our adopted period; the fits listed in Table 3 are for the alias which matches our preferred ephemeris. In general, the less-noisy fits in Table 3 give periods more closely matching the adopted period. As a final check, we split up the first set of H $\alpha$  velocities into two sets according to the state of the system. Performing the period search on each of these sets both produced essentially the same period as the original search on the full data set. Thus we are confident that our period is correct.

#### 4. Conclusion

We have determined the orbital period of HL CMa unambiguously to be 0.2167867(17) d. We also have found no significant differences between spectra taken during standstill, during outburst, and during the unusual outbursting in 2001-2002.

*Acknowledgments.* We would like to thank Bill Fenton, who took a portion of the 2.4m data, as well as Cindy Taylor of the Lawrenceville School, who took the 1.3m data. We gratefully acknowledge support from NSF grants AST-9987334 and AST-0307413. We also thank the MDM staff for their able observing support.

## REFERENCES

Bessell, M. S. 1990, PASP, 102, 1181

Chlebowski, T., Halpern, J. P., & Steiner, J. E. 1981, ApJ, 247, L35

Downes, R. A., Webbink, R. F., Shara, M. M., Ritter, H., Kolb, U., & Duerbeck, H. W. 2001, PASP, 113, 764

Hutchings, J. B., Crampton, D., Williams, G., & Cowley, A. P. 1981, PASP, 93, 741

Kato, T. 2002, Informational Bulletin on Variable Stars, 5243, 1

Schneider, D. P. & Young, P. 1980, ApJ, 238, 946

Shafter, A. W. 1983, ApJ, 267, 222

Still, M. D., Steeghs, D., Dhillon, V. S., & Buckley, D. A. H. 1999, MNRAS, 310, 39

Thorstensen, J. R. & Freed, I. W. 1985, AJ, 90, 2082

Thorstensen, J. R., Fenton, W. H., & Taylor, C. J. 2004, PASP, 116, 300

Thorstensen, J. R., Patterson, J. O., Shambrook, A., & Thomas, G. 1996, PASP, 108, 73

Wargau, W., Drechsel, H., Rahe, J., & Bruch, A. 1983, A&A, 125, L1

Watanabe, T., Stubbings, R., & Maehara, H. 2000, VSOLJ Var. Star Bull., 35-36, 7

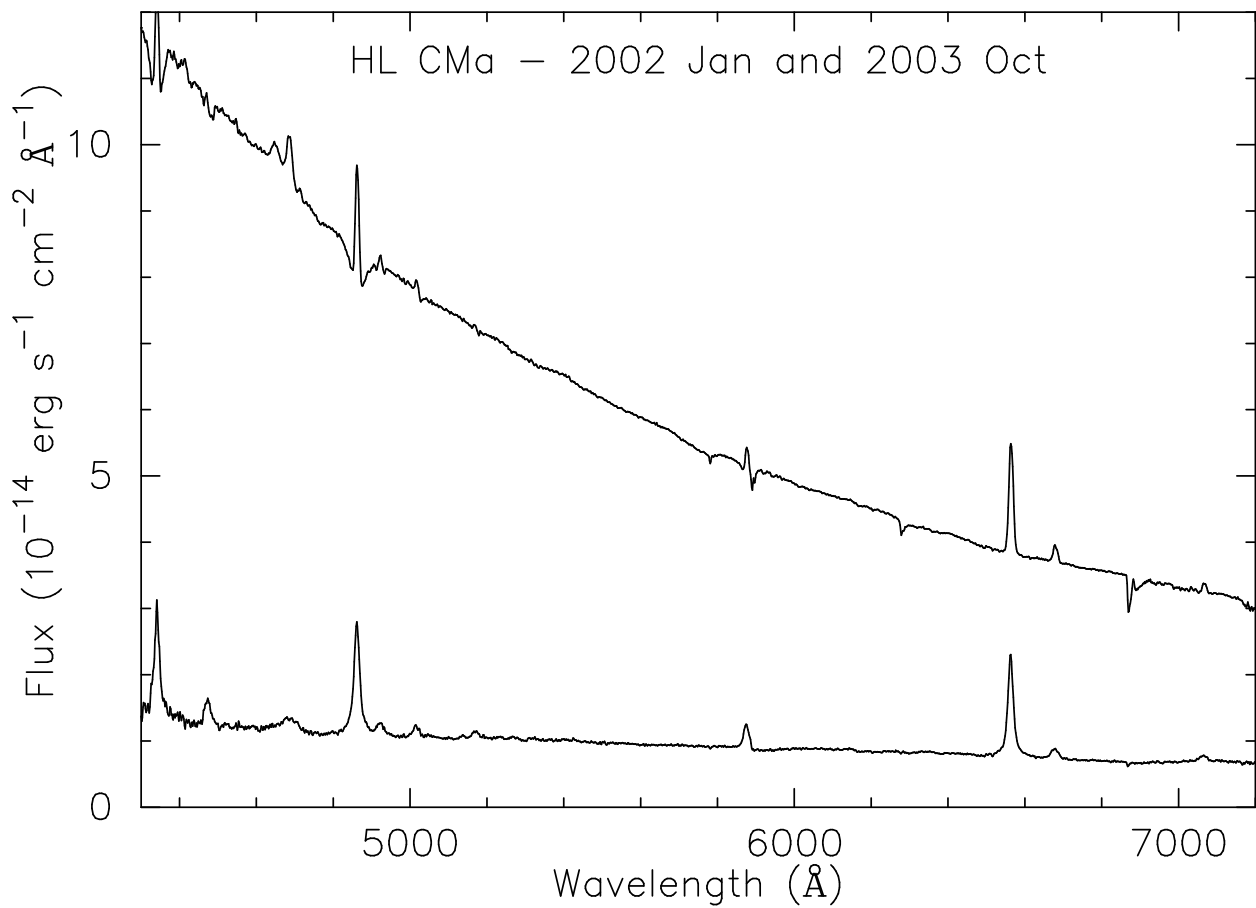


Fig. 1.— The averaged spectra from 2002 January (top) and 2003 October (bottom) are plotted.

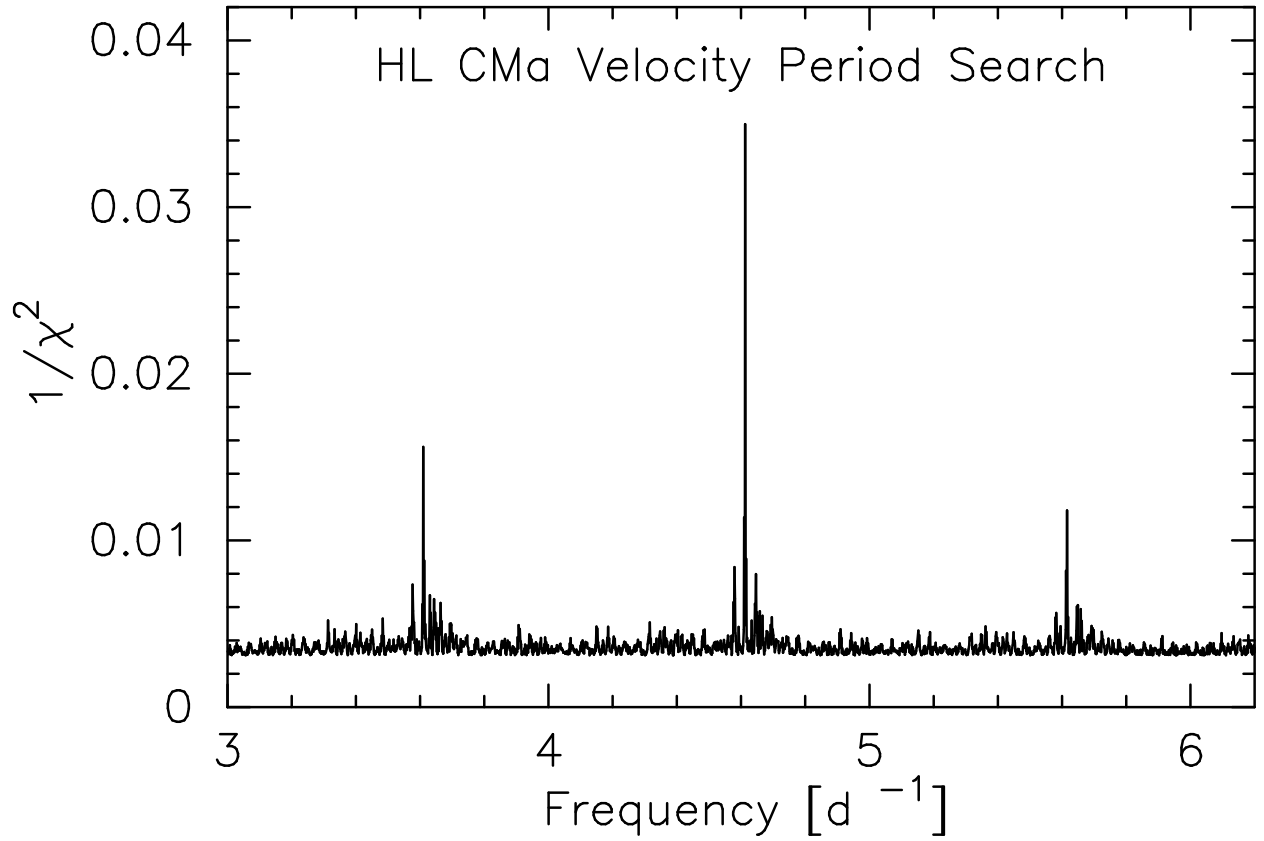


Fig. 2.— The tallest peak, in the center, corresponds with the best fit frequency of 4.61 cycles day<sup>-1</sup>. The two next-best fits are the aliases at 3.61 cycles day<sup>-1</sup> and 5.62 cycles day<sup>-1</sup>. Frequency space is oversampled by a factor of 12 in the original search. This figure was created by plotting the local maxima of the original periodogram and connecting those points with straight lines.

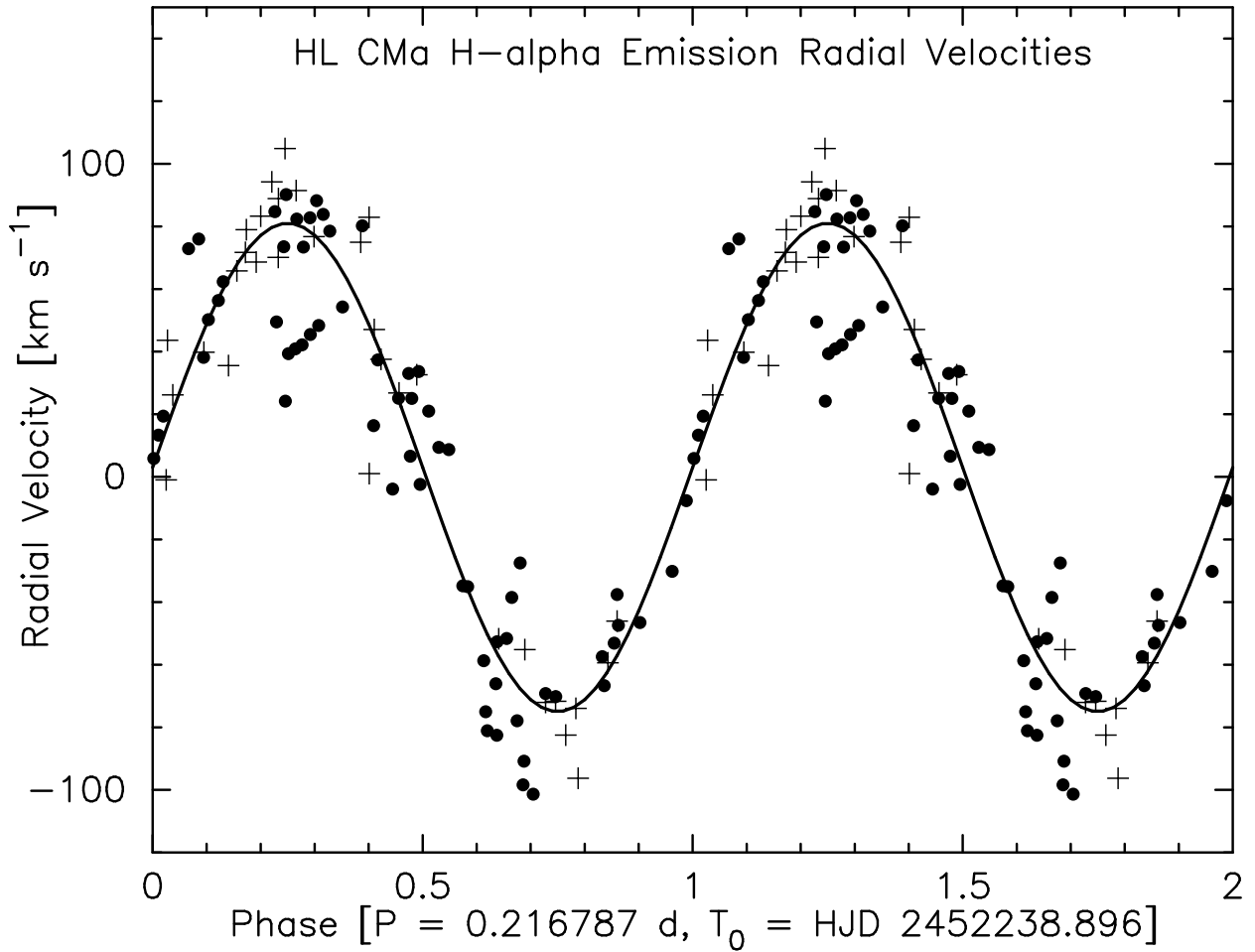


Fig. 3.— Outburst spectra are marked with solid circles, and quiescent spectra are marked with pluses. The data are plotted twice for continuity.

Table 1. Spectral Features in Quiescence and Outburst

| Feature                          | E.W. <sup>a</sup><br>(Å) | Flux<br>( $10^{-16}$ erg cm $^{-2}$ s $^1$ ) | FWHM <sup>b</sup><br>(Å) |
|----------------------------------|--------------------------|--|--------------------------|
| Quiescence - 2003 Oct:           |                          |  |                          |
| H $\gamma$                       | 17.7                     | 2600   | 16                       |
| HeI $\lambda$ 4471               | 5.4                      | 680  | 19                       |
| HeII $\lambda$ 4686 <sup>c</sup> | 8.8                      | 1000   | ...                      |
| H $\beta$                        | 29.2                     | 3400   | 19                       |
| HeI $\lambda$ 4921               | 2.3                      | 260  | 20                       |
| HeI $\lambda$ 5015               | 2.5                      | 230  | ...                      |
| Fe $\lambda$ 5169                | 2.0                      | 210  | ...                      |
| HeI $\lambda$ 5876               | 6.6                      | 600  | 16                       |
| H $\alpha$                       | 37.1                     | 3000   | 18                       |
| HeI $\lambda$ 6678               | 4.1                      | 300  | 21                       |
| Outburst - 2002 Jan:             |                          |  |                          |
| H $\gamma$                       | -1.5 <sup>d</sup>        | -1800  | 10 <sup>e</sup>          |
| HeI $\lambda$ 4471               | 0.1                      | 120  | 7                        |
| CIII/NIII                        | 0.5                      | 450  | ...                      |
| HeII $\lambda$ 4686              | 0.8                      | 790  | 14                       |
| H $\beta$                        | -0.3 <sup>d</sup>        | -290   | 10 <sup>e</sup>          |
| HeI $\lambda$ 4921               | 0.3                      | 240  | 9                        |
| HeI $\lambda$ 5015               | 0.3                      | 200  | 9                        |
| Fe $\lambda$ 5169                | 0.1                      | 46   | 7                        |
| HeI $\lambda$ 5876               | -0.5 <sup>f</sup>        | -240   | 9 <sup>e</sup>           |
| H $\alpha$                       | 6.0                      | 2300   | 13                       |
| HeI $\lambda$ 6678               | 1.0                      | 350  | 13                       |

<sup>a</sup>Emission equivalent widths are counted as positive.<sup>b</sup>From Gaussian fits.<sup>c</sup>Includes weak CIII/NIII blend.<sup>d</sup>Includes the absorption wings.<sup>e</sup>Fit to the emission core of the feature.<sup>f</sup>Includes the absorption wings as well as interstellar Na D absorption, indistinguishable from the wings.

Table 2. Radial Velocities

| Time <sup>a</sup> | $v_{\text{emn}}$<br>(km s $^{-1}$ ) | HA      | Time <sup>a</sup> | $v_{\text{emn}}$<br>(km s $^{-1}$ ) | HA      | Time <sup>a</sup> | $v_{\text{emn}}$<br>(km s $^{-1}$ ) | HA      |
|-------------------|-------------------------------------|---------|-------------------|-------------------------------------|---------|-------------------|-------------------------------------|---------|
| 51549.8790        | −98                                 | +1 : 49 | 52237.8310        | 76                                  | −2 : 06 | 52295.6970        | 13                                  | −1 : 33 |
| 51549.8830        | −101                                | +1 : 55 | 52237.9460        | −81                                 | +0 : 40 | 52295.6980        | 19                                  | −1 : 31 |
| 51641.6120        | −67                                 | +1 : 33 | 52237.9500        | −66                                 | +0 : 45 | 52295.8810        | −47                                 | +2 : 53 |
| 51641.6160        | −53                                 | +1 : 38 | 52238.8600        | −57                                 | −1 : 21 | 52296.8270        | 85                                  | +1 : 39 |
| 51642.6140        | 25                                  | +1 : 40 | 52238.8660        | −38                                 | −1 : 12 | 52297.6460        | 6                                   | −2 : 38 |
| 51642.6180        | 33                                  | +1 : 45 | 52262.8310        | 16                                  | −0 : 29 | 52297.7830        | −83                                 | +0 : 40 |
| 51642.6220        | 34                                  | +1 : 51 | 52262.8390        | −4                                  | −0 : 18 | 52324.6850        | −69                                 | +0 : 06 |
| 51642.6260        | 21                                  | +1 : 57 | 52262.8460        | 7                                   | −0 : 08 | 52324.6890        | −70                                 | +0 : 12 |
| 51642.6300        | 9                                   | +2 : 03 | 52268.6880        | 38                                  | −3 : 32 | 52324.7930        | 49                                  | +2 : 42 |
| 51642.6340        | 9                                   | +2 : 08 | 52268.6950        | 27                                  | −3 : 22 | 52324.7980        | 39                                  | +2 : 49 |
| 51644.6100        | −38                                 | +1 : 42 | 52268.7020        | 33                                  | −3 : 12 | 52325.6640        | 24                                  | −0 : 20 |
| 51644.6140        | −28                                 | +1 : 48 | 52270.8070        | 83                                  | −0 : 32 | 52325.6680        | 41                                  | −0 : 14 |
| 51645.6100        | 42                                  | +1 : 46 | 52270.8140        | 89                                  | −0 : 22 | 52325.7490        | −53                                 | +1 : 43 |
| 51645.6130        | 45                                  | +1 : 50 | 52270.8210        | 91                                  | −0 : 12 | 52325.7530        | −52                                 | +1 : 48 |
| 51645.6170        | 48                                  | +1 : 56 | 52270.8280        | 77                                  | −0 : 02 | 52326.6120        | −75                                 | −1 : 31 |
| 51843.9160        | −1                                  | −1 : 54 | 52293.6300        | 25                                  | −3 : 17 | 52327.6860        | −35                                 | +0 : 20 |
| 51843.9180        | 26                                  | −1 : 52 | 52293.6340        | −2                                  | −3 : 11 | 52327.6880        | −35                                 | +0 : 23 |
| 51992.6790        | 73                                  | +2 : 12 | 52293.7410        | −8                                  | −0 : 37 | 52574.0280        | −47                                 | +0 : 45 |
| 51994.6250        | 94                                  | +1 : 02 | 52293.8190        | 54                                  | +1 : 16 | 52577.0160        | −55                                 | +0 : 40 |
| 51994.6300        | 105                                 | +1 : 09 | 52293.8920        | −91                                 | +3 : 01 | 52620.8660        | −30                                 | −0 : 07 |
| 51995.6150        | −96                                 | +0 : 51 | 52294.6310        | 38                                  | −3 : 12 | 52620.9590        | 80                                  | +2 : 07 |
| 52233.8510        | −72                                 | −1 : 53 | 52294.6330        | 50                                  | −3 : 09 | 52621.8880        | −78                                 | +0 : 29 |
| 52233.8550        | −72                                 | −1 : 47 | 52294.6370        | 56                                  | −3 : 03 | 52624.8140        | 79                                  | −1 : 06 |
| 52233.8590        | −82                                 | −1 : 41 | 52294.6390        | 62                                  | −3 : 00 | 52671.7360        | −59                                 | +0 : 07 |
| 52233.8630        | −74                                 | −1 : 36 | 52294.7010        | 37                                  | −1 : 31 | 52927.0190        | 69                                  | −0 : 15 |
| 52233.9970        | 1                                   | +1 : 38 | 52294.8810        | 90                                  | +2 : 49 | 52927.9840        | −52                                 | −1 : 01 |
| 52234.8610        | 75                                  | −1 : 35 | 52294.8850        | 82                                  | +2 : 55 | 52929.0180        | 47                                  | −0 : 08 |
| 52234.8640        | 83                                  | −1 : 30 | 52294.8880        | 73                                  | +2 : 59 | 53017.8420        | 36                                  | +1 : 23 |
| 52234.9600        | −59                                 | +0 : 48 | 52294.8900        | 83                                  | +3 : 02 | 53017.8460        | 66                                  | +1 : 29 |
| 52234.9630        | −46                                 | +0 : 53 | 52294.8930        | 88                                  | +3 : 06 | 53018.7160        | 72                                  | −1 : 35 |
| 52235.0000        | 44                                  | +1 : 46 | 52294.8950        | 84                                  | +3 : 09 | 53018.7290        | 70                                  | −1 : 16 |
| 52237.8270        | 73                                  | −2 : 12 | 52294.8980        | 79                                  | +3 : 14 | 53066.6090        | 40                                  | −0 : 57 |

<sup>a</sup> Heliocentric Julian data of mid-exposure, minus 2 400 000.

Table 3. Fit to Radial Velocities

| Data set             | $T_0^a$      | $P$<br>(d)    | $K$<br>(km s $^{-1}$ ) | $\gamma$<br>(km s $^{-1}$ ) | $N$ | $\sigma^b$<br>(km s $^{-1}$ ) |
|----------------------|--------------|---------------|------------------------|-----------------------------|-----|-------------------------------|
| H $\alpha^c$         | 52238.896(4) | 0.216787(3)   | 78(7)                  | 3(6)                        | 96  | 19                            |
| H $\alpha^d$         | 52233.912(5) | 0.216787(4)   | 77(10)                 | 7(7)                        | 94  | 24                            |
| H $\beta^e$          | 52233.89(1)  | 0.216795(12)  | 64(17)                 | 2(13)                       | 82  | 40                            |
| H $\beta^f$          | 52233.893(6) | 0.216791(8)   | 66(12)                 | 2(8)                        | 88  | 38                            |
| H $\beta^g$          | 52233.895(8) | 0.216787(9)   | 71(14)                 | 2(10)                       | 93  | 34                            |
| HeI $\lambda 5876^h$ | 52238.867(7) | 0.216786(5)   | 74(14)                 | 7(10)                       | 73  | 46                            |
| HeI $\lambda 5876^i$ | 52233.885(5) | 0.216782(4)   | 87(10)                 | 8(8)                        | 87  | 37                            |
| Weighted Average     | ...          | 0.2167866(17) | ...                    | ...                         | ... |                               |

<sup>a</sup>Heliocentric Julian Date minus 2400000. The epoch is chosen to be near the center of the time interval covered by the data, and within one cycle of an actual observation.

<sup>b</sup>Root-mean-square residual of the fit.

<sup>c</sup>Velocities determined using two gaussians each 3 pixels wide and separated by 7 pixels.

<sup>d</sup>Velocities determined using a derivative of a gaussian 7 pixels wide.

<sup>e</sup>3rd best period, fit to velocities determined using a derivative of a gaussian 4 pixels wide.

<sup>f</sup>2nd best period, fit to velocities determined using a derivative of a gaussian 4.5 pixels wide.

<sup>g</sup>Velocities determined using two gaussians each 2 pixels wide and separated by 4 pixels.

<sup>h</sup>Velocities determined using a derivative of a gaussian 4.6 pixels wide.

<sup>i</sup>Velocities determined using two gaussians each 2 pixels wide and separated by 4.7 pixels.